The American Society of Mechanical Engineers

Reprinted From
HTD — Vol. 106, Heat Transfer Phenomena in Radiation, Combustion, and Fires
Editor: R. K. Shah
Book No. H00498 — 1989

THE RADIATIVE-CONVECTIVE PARTITIONING OF HEAT TRANSFER TO STRUCTURES IN LARGE POOL FIRES

J. T. Nakos and N. R. Keltner
Thermal Test and Analysis Division 7537
Sandia National Laboratories
Albuquerque, New Mexico

I. ABSTRACT

This paper explores the relative contributions of radiative and convective heat transfer to structures (like shipping containers) in large pool fires. Results include measurements of the temperature of two structures (called "calorimeters") in the fire, the flames surrounding the calorimeters, the total heat flux to the calorimeters and the radiative component of the heat transfer at a few locations using transpiration radiometers. These measurements will be compared with calculations. Agreement between the measured radiative heat flux and the calculated radiative heat flux is good. The convective contribution was calculated from the total and radiative parts and was found to be about 10-20% of the total.

II. NOMENCLATURE

h = convective heat transfer coefficient, W/m^2-C
q = heat flux, kW/m^2
T = temperature, C
ε = emissivity
σ = Stefan-Boltzman const., 5.6693×10^{-12} W/cm^2-K^4

Subscripts

c = convective heat flux
er = emitted radiative heat flux
f = flame temperature value
ir = incident radiative heat flux
neti = net flux to surface 'i'
refl = reflected heat flux
si = surface 'i'
t = total = radiative + convective parts

III. INTRODUCTION

This paper explores the radiative/convective partitioning of heat transfer to two calorimeters in a JP-4 (an aviation fuel) pool fire. This is an important consideration in the design of any structural assembly that can be subjected to an accidental fire, because the total heat transfer to that structure and its final temperature will determine whether it can perform its intended function.

In this paper, the general physics of the convective heat transfer mechanism to structures in a turbulent pool fire will be discussed. More complicated phenomena, such as the effects of a participating medium and accelerating flows, are not considered. The convective part of the total heat transfer from a recently completed experiment will be presented and analyzed. Experimental data from a flat plate and a cylinder in cross flow will be analyzed. These are two common configurations of radioactive material shipping containers, so they were used as the modelling configurations for these heat transfer studies. The experimental data from the test includes information from transpiration radiometers and thermocouples mounted on a 3.05 m high vertically oriented flat plate (the "plate calorimeter") and a 1.42 m diameter cylinder (the "cylindrical calorimeter").

The experiments presented in this paper were performed in a fire test facility located at Sandia National Laboratories in Albuquerque, N.M. Tests have been run over a period of several years in a 9 m x 18 m rectangular pool with JP-4 jet fuel floating on water. A variety of shipping containers have been tested simultaneously with other experiments designed to help characterize the fire environment.

IV. LITERATURE REVIEW

The magnitude of the radiative and convective components is important in understanding the total heat transfer to a structure in a fire. The thermal mass, size and shape of the structure will affect that heat transfer. Neill et al. (1970) have studied fires of methanol, acetone, hexane, JP-4, cyclohexane and benzol in circular pans 30.48 cm (12"), 45.72 cm (18") and 60.96 cm (24") in diameter and a cluster burner consisting of 9, 15.24 cm (6") diameter circular pans arranged with one pan in the center and eight pans located 45 degrees apart on 30.48 cm centers. They estimated the convective component to a 11.37 cm diameter, 22.86 cm long vertical cylinder to be from 10-61% of the total heat transfer. From Russell and Canfield (1973), the measured rates of the convective component to a 21.67 cm diameter, 30.48 cm long horizontal cylinder in cross flow ranged from 17-63% of the total in a 2.44 m by 4.88 m (8 ft x 16 ft) pool using JP-5 aviation fuel. Thomas et al. (1965) have estimated the convective part of the total flux to the fuel surface to be from 1/2 of the total at the edge to 1/5 in the center. These measurements were made in wood and ethyl alcohol fires 91 cm in diameter at a location 1-2 cm above the fuel surface. Hamann et al. (1980) modelled the response of a railcar/cask system assuming constant values of the heat transfer coefficient h of 56.8 W/m^2-C and 28.4 W/m^2-C. They obtained the best agreement with experimental data using the lower value for h. Gregory et al. (1987) analyzed the convective heat transfer from a 1.4m diameter flat plate oriented vertically. They found the convective part to be 7% of the total and estimated h to be about 9 W/m^2-C.

There have been many convective heat transfer correlations used in the analysis of fires. Some are standard forced convection correlations taken from heat transfer papers (Russell and Canfield (1973)) and several studies estimate values of the convective heat

transfer coefficient from data taken in a plasma-jet (Ahmed (1968)) and a pool fire (Russell and Canfield (1973)).

The data from Russell and Canfield (1973), which was from turbulent JP-5 pool fire experiments, indicated an average heat transfer coefficient of about 56.1 W/m²-C (9.88 Btu/hr-ft²-F). A correlation was presented and was used to estimate heat transfer coefficients of various gases, presumably those that might be present in a JP-5 fire. The calculated values ranged from 15.3 W/m²-C to 92.0 W/m²-C. This range spans the measured value, but spans it by a rather large amount. For example, if dry air were assumed as the gas present, the calculated value of the heat transfer coefficient would be 15.9 W/m²-C (2.80 Btu/hr-ft²-F); this is 72% below the measured value. Therefore, depending on which gas was assumed present in the fire, the calculated heat transfer coefficient could be significantly different than the actual value.

The highly turbulent free stream conditions may augment the heat transfer coefficient when compared with forced convective heat transfer correlations from flat plates cited in the literature. For example, Drysdale (1985) presented correlations for forced convection that show the transition from laminar to turbulent flow occurs at a Reynolds number of $3x10^5$. However, the free stream flow in our experiments is turbulent at Reynolds numbers near $4x10^4$. This Reynolds number is very close to the value cited by Gregory et al. (1987), i.e. 39,300.

The point to be made is that standard correlations may not be adequate for convective heat transfer calculations in fires. This was also pointed out in Shepherd (1987). One reason that the correlations may not be adequate is that the exact composition of the gas is not known, and in fact changes with time. This would cause property value estimates to be in error. Second, many of the existing correlations are for high Reynolds number turbulent flow at relatively small differences in temperature, whereas in a pool fire the flow is turbulent at low Reynolds numbers and has very high temperature differences. (Ahmed (1968) has shown that standard correlations do need modifications if high temperature differences are present.) Because the convective heat transfer contribution can be more than half of the total, errors in convective coefficients can conceivably have a significant effect on the final results.

V. DESCRIPTION OF CONVECTION IN FIRES

Figure 1 shows several side views of a vertical flat plate. Such a situation would occur if a cylindrical shipping container were oriented upright or if a rectangular container were oriented with one side vertical.

View A shows a situation in which the plate is colder than the surrounding gas and the free stream gas is moving vertically upward, as in a fire. This situation occurs during the early stages of a fire when the object is colder than the surrounding gas. Kent and Schneider (1987) and Schneider and Kent (1989) have shown that the vertical velocities range from an average of about 4 m/s at 2.8 m above the initial pool surface to about 12 m/s at 6.8 m above the surface. Their results also indicate that the flow in these large JP-4 fires is highly turbulent. As a point of comparison, the maximum velocity estimated from natural convection theory from a vertical flat plate 2 m from the leading edge is 2-3 m/sec. This is for a gas at 925C (1700F) and the plate at 38C (100F). In this case, the natural tendency of the fluid near the plate to fall downward is opposed by the "free stream" velocity. Depending on the elevation, the velocities may be roughly the same magnitude. This situation may create several scenarios, two of which are these: 1) the average velocity near the plate may be reduced below the free stream value, which could cause reduced heat transfer or 2) the turbulence may be increased near the plate which could augment the heat transfer mechanism.

View B shows the situation during the middle stages of the fire, after the plate has been heated close to the surrounding gas temperature. Even though there is a free stream velocity flowing upward, there will be little net convective heat transfer because the surface and free stream are at roughly equal temperatures.

Lastly, View C shows the situation that would occur at the end of the fire or during the fire when the winds "tilt" the fire away from the object. In this case the object (650C or 1200F) is hotter than the surrounding gas and there is no free stream velocity. Therefore, the plate will cool only by natural convection.

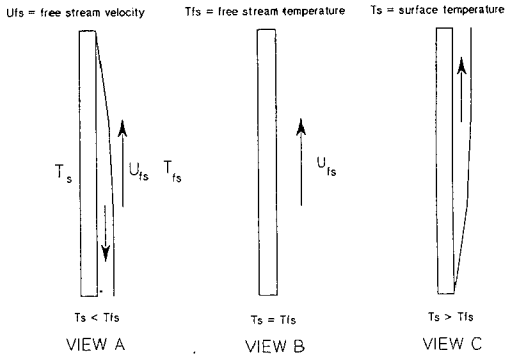

FIGURE 1, CONVECTION PROCESSES IN FIRES

In summary, there are three distinctive convective regimes, depending on the temperature of the structure. These regimes correspond roughly to the early times of the fire, the middle part when the object has reached temperatures close to the flame temperatures and lastly to the end of the fire when the flames have died due to the lack of fuel (or to high winds). During the early regime the free stream is turbulent and moving upward while there is a natural convective force driving gas near the plate downward. The convective heat transfer may be highest during this period. During the middle part of the fire there will be little net convective heat transfer due to the diminished temperature difference. Lastly, after the flames have died, the convective mechanism is purely natural, because the free stream flow has abated.

VI. EXPERIMENT DESCRIPTION

The majority of the experimental data to be presented was gathered from what is called the "plate calorimeter". The plate calorimeter is essentially a heavily instrumented pair of vertically oriented flat steel plates. One plate is 0.48 cm (3/16") thick and is made of 304 stainless steel and the other is 1.91 cm (3/4") thick mild steel. Both plates are about 30.5 cm wide and 305 cm long. They are mounted side by side. Thermocouples were mounted on the front and back faces of the plates and just in front of the plates to measure the flame temperature. In addition, there were two transpiration radiometers mounted on the front face of the plates to measure the incident radiative component of the heat flux. Figures 2 and 3 show an overall view and a sectional view of the plate calorimeter.

Limited data will be presented from a "1.4 m diameter cylindrical calorimeter"; it is described in Gregory, et al. (1987). Figure 4 shows a side view of the 1.4 m diameter cylindrical calorimeter. The calorimeter is 1.4 m diameter and 6.4 m long. The walls are 3.18 cm (1-1/4") thick and are made of A517 steel

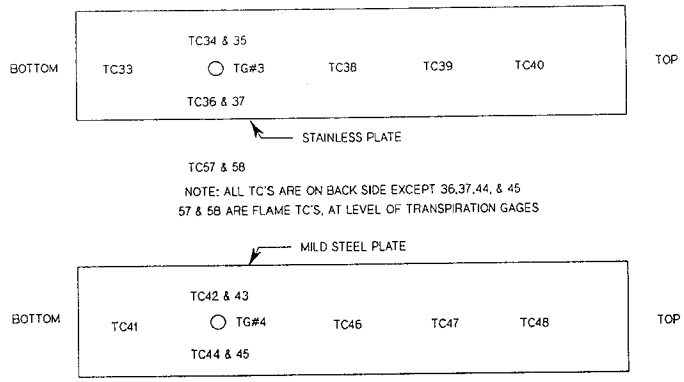

FIGURE 2, FRONT VIEW OF PLATE CALORIMETER

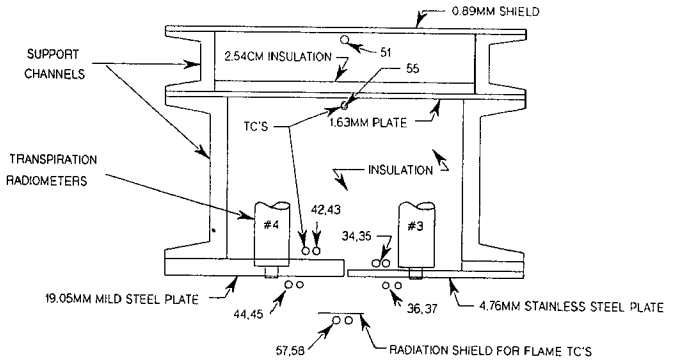

FIGURE 3, SECTION THROUGH PLATE CALORIMETER

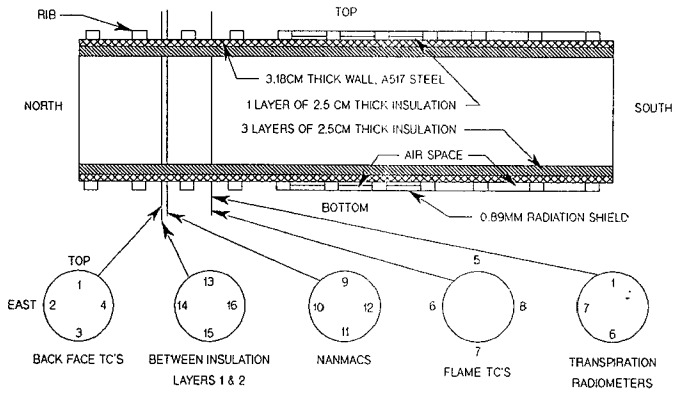

FIGURE 4, SIDE VIEW OF 1.4M DIA. CALORIMETER

with strengthening ribs every 61 cm. Mounted in the 1.4 m calorimeter were transpiration radiometers and thermocouples. Measurements included flame temperatures, temperatures on the backface of the 3.18 cm thick walls and pencil probe "eroding" thermocouples used to measure outer surface temperatures on the calorimeter.

The layout of the pool is shown in Figure 5. The long axis of the pool is oriented in the east-west direction. The test unit, a shipping container, was located on the east side and the 1.4 m diameter calorimeter was located on the west side. The long axis of the test unit was oriented east-west while the long axis of the 1.4 m calorimeter was oriented north-south. The plate calorimeter was placed between the test unit and the 1.4 m cylindrical calorimeter. It was placed north of the centerline of the pool. The side of the calorimeter that contained the transpiration gages faced to the south, into the fire. As indicated in Figure 5, there were other experiments in the pool, but those results will not be presented here. The entire 9m x 18m area of the pool was filled with JP-4 fuel to a depth of about 20 cm (8"). This amounted to about 33,000 liters (8,800 gal) of fuel.

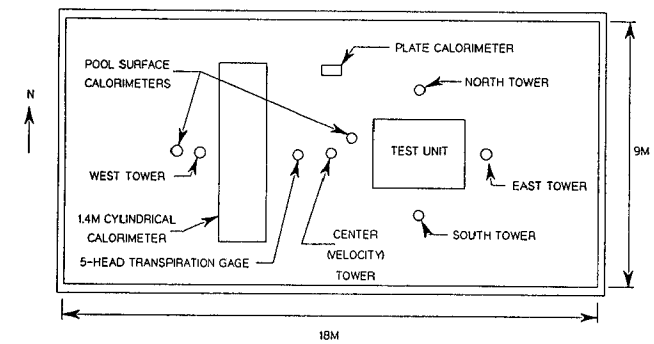

FIGURE 5, 9M X 18M POOL LAYOUT

VII. ANALYSIS

Calculation of the convective heat transfer component has its basis in the following energy balance:

$$q_{net} = q_{ir} - q_{er} + q_c - q_{refl}, \quad (1)$$

where q_{net} = net absorbed heat flux, q_{ir} = incident radiant flux, q_{er} = emitted radiative flux, q_c = convective heat flux, and q_{refl} = reflected radiative flux. An energy balance for surface 'i' can be written as follows:

$$q_{neti} = \sigma\varepsilon_f T_f^4 - \sigma\varepsilon_{si} T_{si}^4 + h_{si}(T_f - T_{si}) - (1-\varepsilon_{si})\sigma\varepsilon_f T_f^4, \quad (2)$$

The above relation assumes that the shape factors are equal to 1.0 and that the surface absorptivities equal the surface emissivities. Subscripts 'net' refer to net absorbed values, 'f' to flame temperature values, and 'si' to 'surface i'.

Solving (2) for the convective component gives:

$$h_{si}(T_f - T_{si}) = q_{neti} + \sigma\varepsilon_{si} T_{si}^4 - \sigma\varepsilon_{si}\varepsilon_f T_f^4. \quad (3)$$

Equation (3) can be used to estimate the convective heat transfer to surface 'i' from the measured flame temperatures, surface temperatures and the absorbed heat flux. The net absorbed heat flux was estimated from the backface temperature measurements by using an inverse heat conduction algorithm called SODDIT (Blackwell et al. (1987)). SODDIT also estimates the front face temperature and so these values can be compared with measured values from the "eroding" thermocouples and 1.59 mm (1/16") diameter sheathed thermocouples.

Writing equation (2) for the stainless and mild steel plates, subtracting one from the other and rearranging gives:

$$h = [q_{net1} - q_{net2} - \sigma\varepsilon(T_{s2}^4 - T_{s1}^4)]/[T_{s2} - T_{s1}]. \quad (4)$$

This equation assumes that the heat transfer coefficients for both plates are the same, which is not true if the plate temperatures are significantly different. It was also assumed that the flow fields on the two plates were the same, for example, similar to that shown in either View A or B in Figure 1. Equation (4) can be used to estimate the convective heat transfer coefficient, as long as the temperature difference $[T_{s2} - T_{s1}]$ is not zero and as long as the coefficients h_{s1} and h_{s2} are equal. In equation (4), ε_{s1} and ε_{s2} were made the same by painting both steel surfaces with a high absorptivity paint, Pyromark Black. Similarly, equation (3) for each surface can be used to estimate the convective heat transfer coefficient h. There is at least one advantage in using the equation (4) over equation (3), to calculate h. Flame temperatures are used in equation (3), as are assumed values for flame emissivity. Flame temperatures are measured, but flame emissivity values are not. In addition, flame temperatures fluctuate considerably and are measured only at a point several inches out from the plate surface. As a result, that flame temperature measurement may not be an accurate indication of the effective temperature of the radiation source to the plate surface. The use of equation (4) eliminates the need for flame temperatures or emissivities, which could have large errors, and so is presumably more accurate. However, the use of (4) to determine h could also have problems, including possibly a different frequency content of the temperature data and total absorbed heat flux data (q_{net1} and q_{net2}) for the two thicknesses of the plates. In addition, if the temperature difference $[T_{s2} - T_{s1}]$ becomes small, the coefficients h_{s1} and h_{s2} are not equal or the flow fields are not the same, the calculations for h would not be valid.

The total heat flux incident on the front surface can be estimated from the sum of the radiative and convective parts ($q_t = q_{ir} + q_c$), which, from equation (2), gives the following relation:

$$q_t = q_{neti} + q_{er} + q_{refl} = q_{neti} + \sigma\varepsilon_{si} T_{si}^4 + (1-\varepsilon_{si})\sigma\varepsilon_f T_f^4 \quad (5)$$

The net absorbed flux, q_{neti}, is calculated from SODDIT. The convective, radiative and total heat fluxes are calculated separately in a small program written for these calculations.

Note that, as defined, the total flux can be less than the radiative flux. The fluxes are defined as positive if they go into the surface, negative if they are outgoing.

From the ratio of the total and convective parts of the heat

transfer, the convective contribution can be obtained as a function of time during the fire. Lastly, the calculated radiative contribution can be compared with the measured radiative contribution obtained from the transpiration gage data.

VIII. RESULTS

Data from three of the transpiration radiometers are shown in Figures 6-8. In Figures 6 & 7, the radiative heat fluxes incident on the mild steel (MS) and stainless steel (SS) sides of the plate calorimeter are shown. One would expect that the output of gages #4 & #3 (Figures 6 & 7) would be close, since they are only about 0.6 m apart. This is the case until about the 27 minute time, when the output of gage #3, Figure 7, starts to drop. Perhaps the gage surface was affected by soot buildup, because there was a considerable negative offset after the fire was out. Some of the gages did have soot buildup after the test, even though the buildup should have been minimal due to the transpiration gas flow. The exact cause(s) of this offset are not known at this time. However, gage #4, Figure 6, shows very little offset at either the beginning or the end of the test.

Figure 8 shows the heat flux (looking upward) on the top of the 1.4 m cylindrical calorimeter. The two other radiometers on the cylindrical calorimeter produced data with large offsets at the end of the test, and so those data are not shown. The output from the gage on the top of the 1.4 m calorimeter was modified because the actual transpiration gas flow rate during the test was not the same as that used in the calibration of the gage. Because the gage output is highly sensitive to the flow rate of the gas (Matthews et al. (1986)), the output at the lower flow rate was higher than the calibration values. Gage #1, Figure 8, showed some offset after the test, but not as much as gage #3.

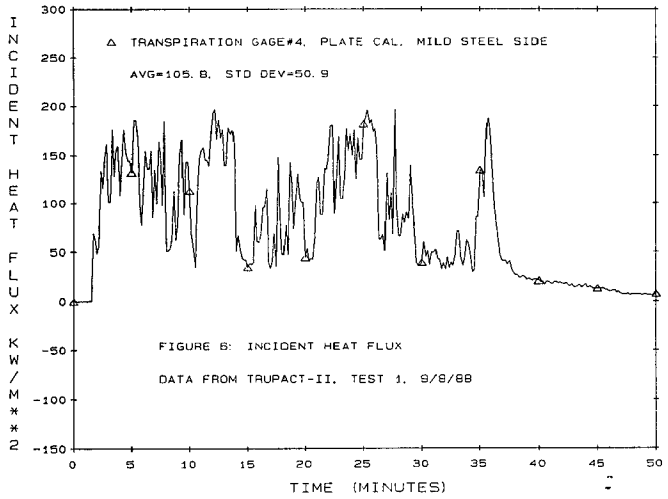

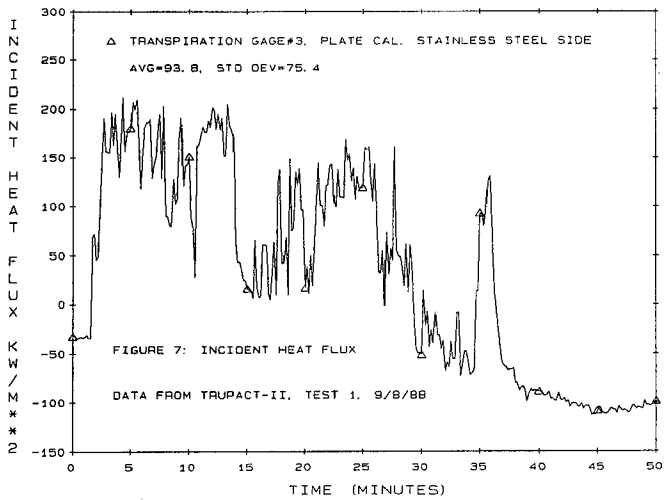

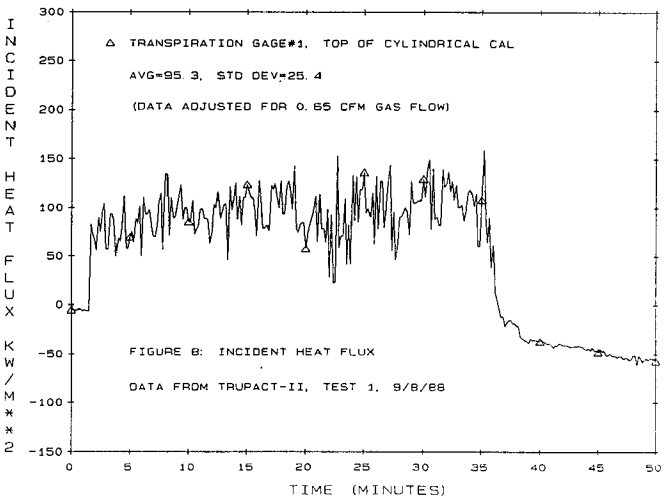

The average values and standard deviations of all 3 gages from 3 to 33 minutes are also shown on the figures. They range from 93.8 to 105.8 kW/m^2. Remember that the output from gage #1 was modified to account for the low transpiration gas flow rate, and therefore the results shown in Figure 8 are subject to larger uncertainties than those in Figures 6 & 7.

Figure 9 shows the radiative heat flux near the plate calorimeter calculated from the flame temperatures, which were measured with two thermocouples located at the junction of the two steel plates. The outputs of the two thermocouples were almost identical. As noted on the figure, the assumed value for the flame emissivity was 0.82. This value was obtained by varying the average value of the flame emissivity until the average radiative heat flux calculated by the equation $\sigma\varepsilon_f T_f^4$ was the same as that obtained from the transpiration radiometer shown in Figure 6. As can be seen, the average values shown in Figures 6 and 9 are almost identical. In addition, if one overlays these two plots, the calculated and measured radiative heat fluxes show good agreement.

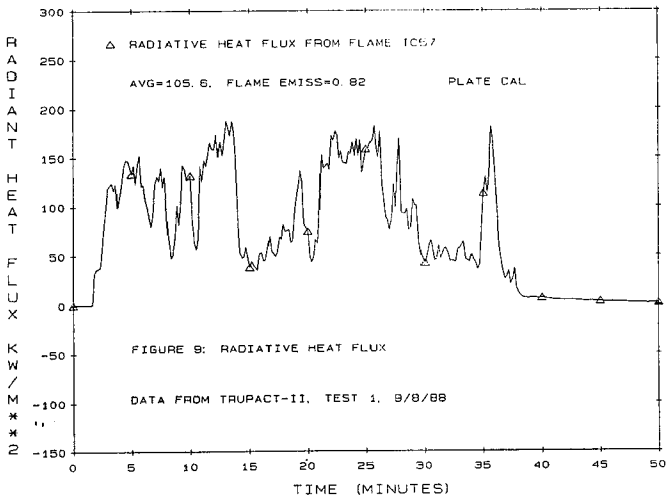

Figures 10 & 11 show the total heat fluxes (from equation (5)), the radiative fluxes (from the flame temperatures), and the convective fluxes (from equation (3)). As can be seen, the average convective flux on the mild steel (MS) side is about 14.8 kW/m^2, or about 12.3% of the total. For the stainless steel (SS) side, the average convective flux is about 22.0 kW/m^2 or 17.3% of the total.

Figures 12 & 13 show front face temperatures and the flame temperature from TC57. Note that the front face temperatures shown were generated from SODDIT. These were compared with the measured front face temperatures and the agreement was very good. Figure 14 shows a typical plot. A sheathed thermocouple mounted on the front surface of a steel plate and subjected to a radiant heat flux will read higher than the surface to which it is

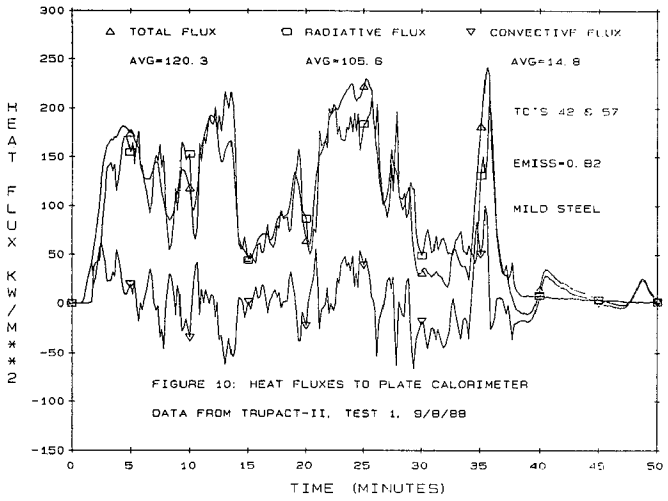

FIGURE 10: HEAT FLUXES TO PLATE CALORIMETER

DATA FROM TRUPACT-II, TEST 1, 9/8/88

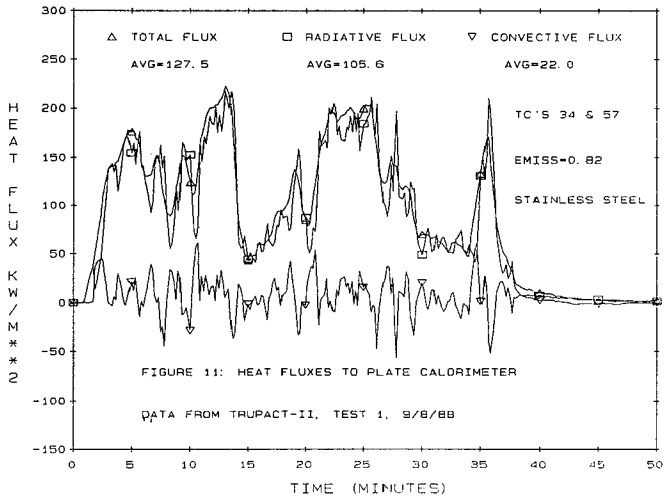

FIGURE 11: HEAT FLUXES TO PLATE CALORIMETER

DATA FROM TRUPACT-II, TEST 1, 9/8/88

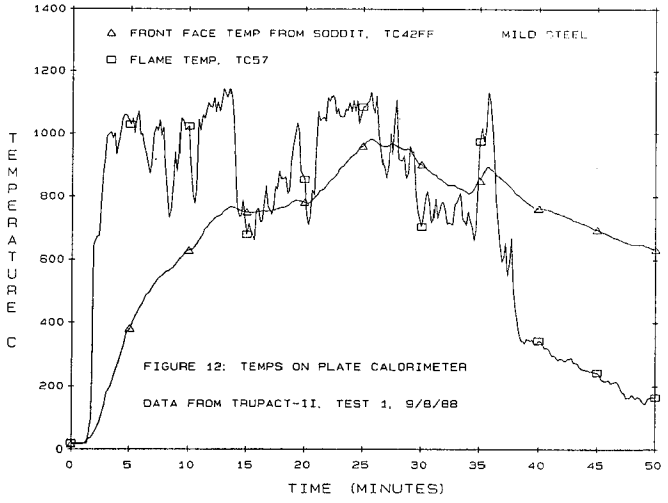

FIGURE 12: TEMPS ON PLATE CALORIMETER

DATA FROM TRUPACT-II, TEST 1, 9/8/88

attached. This trend is evident from the data in Figure 14. As a result, it was decided that the calculated front face temperatures are preferred, and these were used in Figures 12 and 13.

It is instructive to compare the heat flux plots in Figures 10 and 11 with the temperature plots in Figures 12 and 13. Note in Figure 12 that from the very beginning of the test to a time of about 13-14 minutes, the flame temperature was higher than the surface temperature of the mild steel plate. As a result, the convective flux, defined as $h(T_f - T_s)$, would be positive. This scenario was discussed in Section IV and shown in Figure 1, View

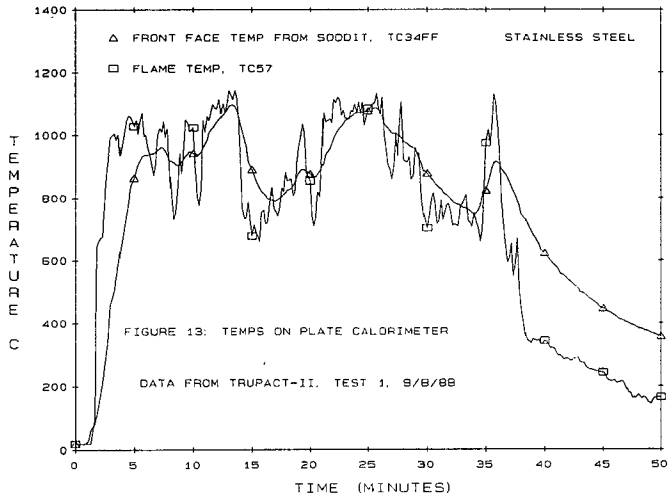

FIGURE 13: TEMPS ON PLATE CALORIMETER

DATA FROM TRUPACT-II, TEST 1, 9/8/88

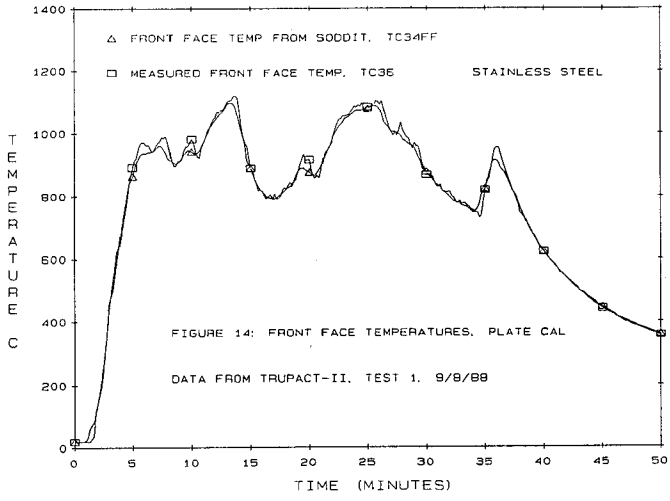

FIGURE 14: FRONT FACE TEMPERATURES, PLATE CAL

DATA FROM TRUPACT-II, TEST 1, 9/8/88

A. During 14-20 minutes, the flame and plate temperatures are close, and so the convective flux should be small (View B). From about 21-26 minutes the flames are again hotter than the plate and so the convective flux should be positive. From about 26-34 minutes the two temperatures are close and so the convective flux should be small. Lastly, the spike at about 35 minutes again brings the flame temperature above the plate temperature and so the convective flux should be positive. A close scrutiny of the plot in Figure 10 shows the general trends just outlined.

Similar trends are difficult to establish on the stainless steel side (Figures 11 and 13) because the plate temperature and flame temperatures were much closer throughout the test, except at the very beginning. The stainless steel plate is much thinner than the mild steel plate and so responds faster.

Figures 15 and 16 show heat flux data from the 1.4m diameter cylindrical calorimeter. Figure 15 shows the calculated radiative heat flux from TC5 assuming a flame emissivity of 0.82. The average of this plot is about 116.4 kW/m², which is 20% above the average value of 95.3 kW/m² from the radiometer data shown in Figure 8. This discrepancy is not surprising because the radiometer data were corrected for the low transpiration gas flow rate in a very approximate manner and the correction may not be accurate. However, the general trends in Figures 8 and 15 are similar.

The calculated total, radiative and convective fluxes on the top of the cylindrical calorimeter are shown in Figure 16. As can be seen, the average value of the convective part is 15.1 kW/m² or about 11.5% of the total. This contribution is on the low side of those reported in Russell and Canfield (1973) for a small cylinder (17-63%).

Figure 17 shows the flame temperature and front face temperature on the top of the 1.4m diameter calorimeter. As can be seen, the flame temperature is greater than the surface

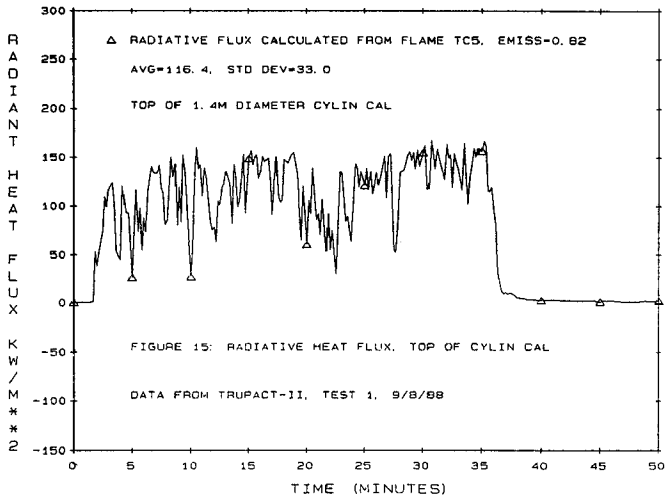

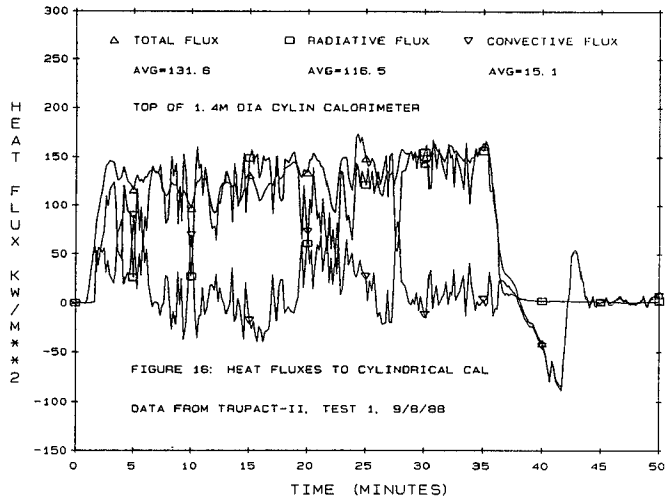

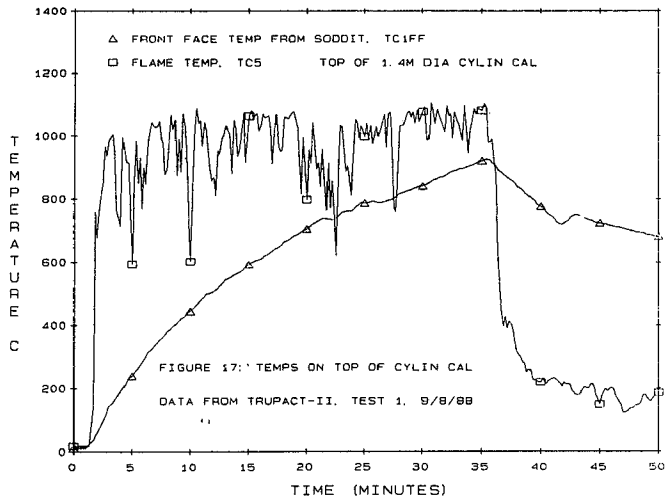

temperature through most of the test. As a result, the convective flux should be positive for most of the test, and this is generally the case (see Figure 16). However, during the 7-20 minute time, the convective component seems more negative than positive. The convective flux also seems to decrease towards the end of the test, as would be expected since the temperature difference decreases steadily. Lastly, note that the convective flux drops to almost -100 kW/m^2 after the fire is over. This would be expected because the hot cylinder would generate a natural convective heat loss to the cooler environment, as shown in View C, Figure 1.

The periods of negative convective heat flux in Figure 16 could be due to an overestimation of the flame emissivity and/or surface absorptivity or the fact that the flame thermocouple, TC5, was located about 0.55 m laterally away from the location of the back face thermocouple. Due to this separation, using TC5 to calculate the radiative heat flux may not be accurate. Using a flame emissivity or surface absorptivity that is too high would result in an overestimate of the radiative component and therefore an underestimate of the convective component. All of these factors contribute to the uncertainty of these calculations and could have caused the negative convective flux during the 7-20 minute time period.

Some results, based on equations (3) and (4), were generated for the convective heat transfer coefficient h. The results produced from equation (3) were oscillatory in nature and grew in magnitude with increasing time. The results produced from equation (4) seemed unreasonably high and are most likely due to the fact that the measurements were not sufficiently accurate. After the first 4 minutes the plate temperatures were at least 400 C different, the thinner stainless steel plate having heated faster. Therefore, one could not assume that h_{s1} and h_{s2} were equal and the assumptions used in the derivation of equation (4) are not valid. In the future, modifications will be made to the general setup that could improve the results.

IX. CONCLUSIONS

Several conclusions can be drawn from the above discussions and results:

1) Using transpiration radiometers and flame temperatures, one can compare to reasonable accuracy (20%) the radiative component using an assumed flame emissivity of 0.82 (for this test only).

2) The average convective contribution of the total heat transfer is from 10-20% of the total, which says that the radiative component is by far the largest part.

3) One can use front face temperatures calculated from the inverse heat conduction program SODDIT with good accuracy. This eliminates the need for many expensive measurements.

X. ACKNOWLEDGEMENTS

The authors would like to thank W.R. Jacoby, J.T. Meloche, B.G. Strait and L.A. Kent for their support in the fabrication, data acquisition and data reduction of the work presented in this paper. Special thanks go to Jerry Meloche for the overall test setup, to Bill Jacoby for the detailed fabrication of the plate and cylindrical calorimeters, to Bob Strait for the conscientious calibration of the data acquisition system and to Larry Kent for data reduction. Sandia National Laboratories is operated by AT&T Technologies for the U.S. Department of Energy (DOE) under Contract DEAC0476DP00789.

XI. REFERENCES

Ahmed, A.M., "Forced Convective Heat Transfer to Cooled Cylinders at Low Reynolds Numbers and with Large Temperature Differences", Canadian Armament Research and Development Establishment Technical Report 588/68, Sept., 1968.

Blackwell, B.F., Douglass, R.W., Wolf, H., "A Users Manual for the Sandia One-Dimensional Direct and Inverse Thermal (SODDIT) Code", SAND85-2478, May, 1987.

Drysdale, D., An Introduction to Fire Dynamics, J. Wiley & Sons, 1985, pg 56.

Gregory, J.J., Keltner, N.R., and Mata, R., Jr., "Thermal Measurements in Large Pool Fires", Heat and Mass Transfer in Fires, ASME-HTD-VOL. 73, pp 27-36, 1987. (To be published in the Journal of Heat Transfer.)

Hamann, J.E., Klein, D.E., Pope, R.B., and Yoshimura, H.R., "Modelling of Pool Fire Environments Using Experimental Results of a Two-Hour Test of a Railcar/Cask System", 6th International Symposium on the Packaging and Transportation of Radioactive Materials (PATRAM), 1980, pp 1081-1089.

Kent, L.A., and Schneider, M.E., "The Design and Application of Bi-Directional Velocity Probes for Measurements in Large Pool Fires", ISA Transactions, Vol. 26, No. 4, 1987.

Matthews, L., Longenbaugh, R., and Mata, R., "Transpiration Radiometer in Fire Characterization", InTech, ISA, August, 1986.

Neill, D.T., Welker, J.R., Sliepcevich, C.M., "Direct Contact Heat Transfer from Buoyant Diffusion Flames", J. Fire & Flammability, Vol.1, October, 1970, pp 289-301.

Russell, L.H., Canfield, J.A., "Experimental Measurement of Heat Transfer to a Cylinder Immersed in a Large Aviation-Fuel Fire", J. Heat Transfer, August, 1973, pp 397-404.

Schneider, M.E., and Kent, L.A., "Measurements of Gas Velocities and Temperatures in a Large Open Pool Fire", Fire Technology, Vol. 25, No. 1, Feb., 1989, pp 51-80.

Shepherd, J.E., "Analysis of Diffusion Flame Tests", Sandia National Laboratories Report SAND86-0419, 1987.

Thomas, P.H., Baldwin, R., and Heselden, A.J.M., "Buoyant Diffusion Flames: Some Measurements of Air Entrainment, Heat Transfer, and Flame Merging", Tenth Symposium (International) on Combustion, The Combustion Institute, 1965, pp 983-996.